Chapter 4: Stress

STRESS IS a quantity perceived by many students to be more difficult to comprehend than force. This may partly be attributable to the tensor nature of stress. Stress is a tensor quantity, specifying the magnitude and direction of the tensional, compressional, and shear forces per unit area in a point of a particular material plane. The tensor notation employs double suffixes to distinguish the various types of stresses and their orientation with respect to a particular coordinate system (σ_{xx}, σ_{xz}, etc.). However, for an initial understanding of stress, it is not necessary to introduce the stress tensor directly. This section considers only the so-called *principal stresses*, which are denoted by single suffixes. The mathematical concept of the stress tensor is not introduced until chapter ten.

Practical hint: **Invaluable comprehension of stress quantities may be established by performing in-situ stress measurements, either indoors or outdoors.**

Contents: The stress ellipsoid is introduced in section 4-1. The fundamental difference between the deviatoric and total stress and their interrelationships is explained in section 4-2. That simple vector calculus is not valid for stress quantities is emphasized in section 4-3. The relationship between principal stresses and normal and shear stress components can be derived, taking into account the area for the different stress orientations, as shown in section 4-4. Consequently, the force vector and the major principal stress are usually *not* parallel, as demonstrated in section 4-5. The concept of stress trajectories and their application to geological intrusions is outlined in section 4-6. Finally, some practical field methods for in-situ stress measurements are summarized in section 4-7.

4-1 Stress ellipsoid & sign conventions

In three dimensions, stress can be graphically and mathematically represented by a *stress ellipsoid*, using three principal stresses (Fig. 4-1a). These stresses are mutually perpendicular, and the length of the respective axes is proportional to their relative magnitude. The stress ellipsoid comprises three mutually perpendicular ellipse sections, each containing two of the three principal stress axes (Fig. 4-1b to d). The ellipsoid representation requires that both the orientation and magnitude of the principal stresses are known. These requirements may be impractical for some natural situations, where the stress parameters may not be available. Nonetheless, principal stresses can be considered as the master stresses, with a particular orientation in space, which completely determine the state of stress in a point, independent of any coordinate system. The equation for the stress ellipsoid, with the coordinate axes (X,Y,Z) taken parallel to the principal stresses, σ_1, σ_2, and σ_3, is:

$$(\sigma_x/\sigma_1)^2+(\sigma_y/\sigma_2)^2+(\sigma_z/\sigma_3)^2=1 \qquad (4\text{-}1)$$

with ellipsoid tracer coordinates $(\sigma_x,\sigma_y,\sigma_z)$. The principal stresses are *always* mutually perpendicular, so that there are two principal stresses in two dimensions and three principal stresses in three dimensions (Fig. 4-1). The suffixes are conventionally chosen, such that stress magnitudes are ranked according to $|\sigma_1| > |\sigma_2| > |\sigma_3|$. The absolute stress magnitudes are deliberately taken here for the suffix ranking, because of some contradictory sign conventions.

In this book, rock mechanics and continuum mechanics are combined. However, these disciplines follow different *sign conventions*. The convention in physics and engineering is to take compressional stresses negative and tensional stresses positive. Conversely, in geology and rock mechanics the literature commonly uses a sign convention which defines compressional stresses as positive. The latter convention may easily lead to computational inconsistencies in finite strain calculations from dynamic equations including stresses for the forward modeling of rock deformation. The mechanical engineering sign convention is adopted here, unless stated otherwise.

☐Exercise 4-1: The 2D section of the stress ellipsoid in the XZ-plane reduces equation (4-1) to that of a stress ellipse: $(\sigma_x/\sigma_1)^2+(\sigma_z/\sigma_3)^2=1$. Sketch, to scale, the pressure circle and total stress ellipse in a point with P=-100 MPa, σ_1=-150 MPa, and σ_3=-50 MPa.

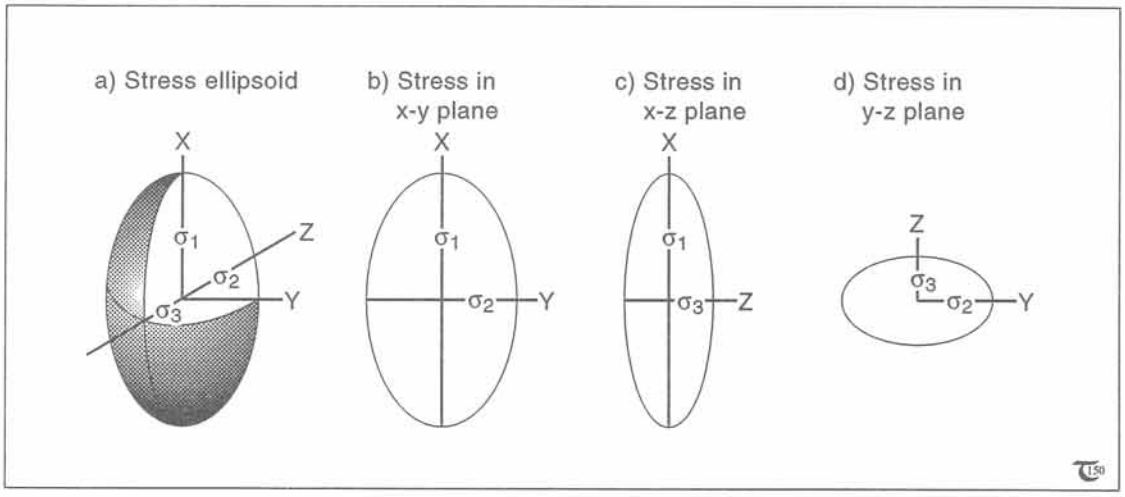

Figure 4-1: *a) The stress ellipsoid. Sections b) to d) are the stress ellipses, representing the state of stress in the principal planes.*

4-2 Total and deviatoric stress

Stress is perceived as such a complex quantity by many students, not only because of its direction-dependent properties, but, also, because there are *two types of principal stresses*: *total stresses* and *deviatoric stresses*. Throughout this book, total stresses are denoted by σ and deviatoric stresses by τ. Normal and shear stresses will be distinguished by either single subscripts, e.g., σ_N and σ_S, respectively, or double subscripts when using tensor notation, e.g., σ_{xx} and σ_{xz} (see chapter ten).

The total stress includes both a pressure and deviatoric stress. The deviatoric stress is free from any pressure contribution and causes distortion of shape, whereas pressure may cause only potential volume change. In other words, the pressure is the difference between the deviatoric and total stresses. Any constitutive equation, governing either elastic deformation or ductile creep, involves the deviatoric stress, because the pressure component in the total stress is not contributing to any distortion without volume change.

Pressure and stress are related as follows: The pressure induced by a total stress in any point is equal to the mean of the total principal stresses in that point:

$$P=\sigma_{mean}=(1/3)(\sigma_1+\sigma_2+\sigma_3) \qquad (4\text{-}2a)$$

or in two dimensions:

$$P=\sigma_{mean}=(1/2)(\sigma_1+\sigma_3) \qquad (4\text{-}2b)$$

Pressure is sometimes considered as a reactive force acting opposite to compression, in which case pressure is positive and the use of absolute values of P in eqs. (4-2a & b) may be preferred.

Principal deviatoric stresses, $\tau_{1,2,3}$, resulting when any of the principal total stresses differ from P, can be directly calculated from:

$$\tau_{1,2,3}=\sigma_{1,2,3}-P \qquad (4\text{-}3)$$

The difference between τ, σ, and P may be clarified, considering their respective role in a small party balloon inflated with air (Fig. 4-2a). The balloon's elastic shell deforms if subjected to a total external stress, σ_1. The pressure inside the elastic shell will increase by a particular amount, P_σ, due to the application of σ_1. However, the balloon's deformation is the result of the deviatoric component of the total stress, i.e., $\tau_1=\sigma_1-P_\sigma$. The total stress balances the sum of the deviatoric stress and the induced pressure (P_σ). The direction of the *stress arrows* may indicate compression or tension. The principal axes of the deviatoric and total stresses coincide at all times, but Figure 4-2b emphasizes that all arrows of the total principal stresses point in the same direction (here compressional), whereas those of the devia-

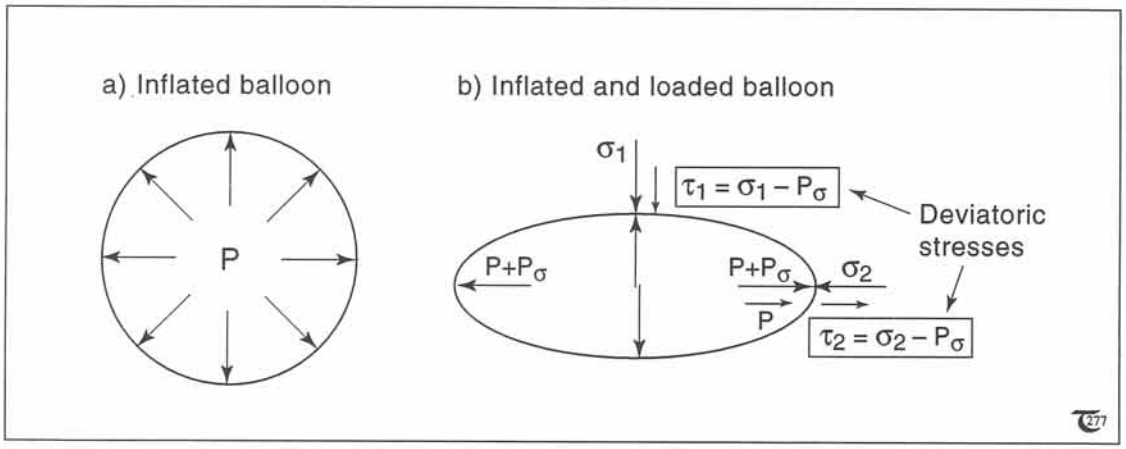

Figure 4-2: *a) Principle sketch of the pressure inside a stress-free balloon. b) Total stress and deviatoric stress both exist when an external surface force is applied.*

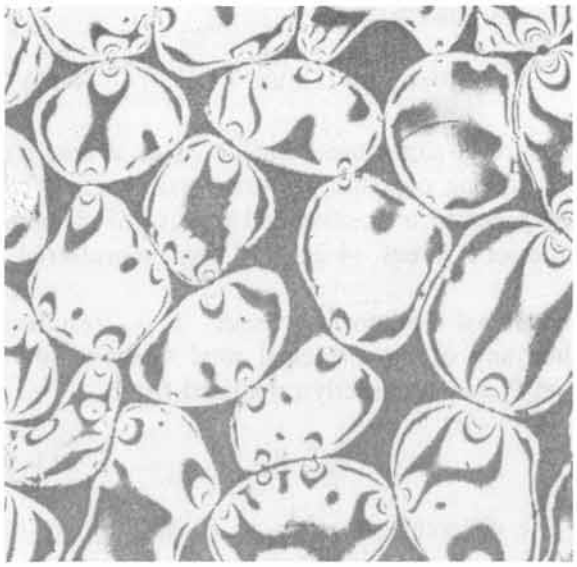

Figure 4-3a: *Photoelastic fringes of polarized light, transmitted through aggregate of plexiglass grains. The fringes are contours of equal deviatoric shear stress magnitude.*

toric stress point in mutually opposite directions (τ_1 is compressional; τ_2 is tensional). *The deviatoric stress arrows accurately indicate the direction of material displacement, if any, associated with the distortion of shape.*

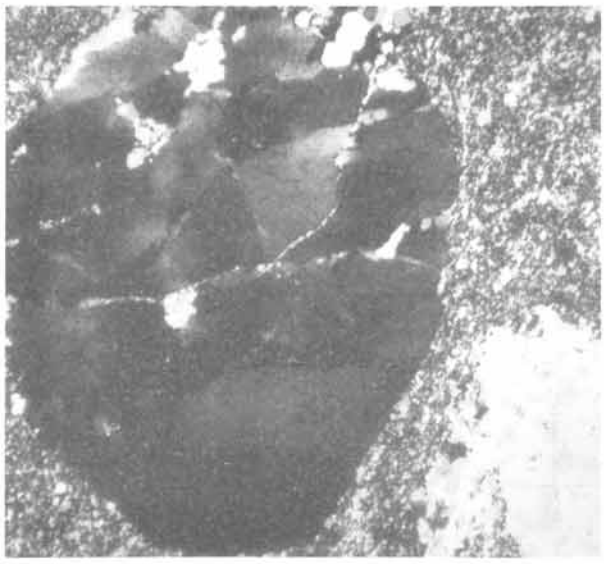

Figure 4-3b: *Crushed clast of quartz in polymict sandstone aggregate. Courtesy Håkan Sjöström.*

If there is no deviatoric stress, the total stress is sometimes called *neutral* or *isotropic*, implying the absence of any real stress (or tensor quantity), and only a pressure (scalar quantity) occurs. It should be noted, again (cf. section 3-5), that some schools avoid to term the mean lithostatic stress a pressure. They follow the assumption that any time a rock is buried, it is subjected to a stress regardless of whether or not the principal stresses are equal. In this assumption, the mean stress may be taken equal to the pore pressure.

Gradients of deviatoric stress can be visualized in materials like plexiglass, which are photoelastic. Figure 4-3a shows an aggregate of plexiglass pellets, a good analog for porous and granular sedimentary rocks at shallow depths, and visualizes the deviatoric stress distribution inside the vertically loaded grains. Shear stresses can exist only if there is deviatoric stress, and vice versa. The isochromatic fringe patterns of polarized light outline surfaces, where the magnitude of the *maximum shear stress*, τ_S, for individual material points is equally large:

$$\tau_{S\,max} = (1/2)(\tau_1 - \tau_3) = \text{constant} \qquad (4\text{-}4)$$

In Figure 4-3a, the deviatoric stresses are largest in the center of the grains, as can be inferred by comparison with the scaled trajectories of the normally loaded sample of Figure 6-5 (see chapter six).

The deviatoric stress inside the grains of Figure 4-3a occurs partly because there is no fluid in the pore space between the grains. If a pore fluid were present, and if the fluid pressure were sufficiently large, the deviatoric stress in the grains may vanish altogether. On the other hand, grains will be crushed (Fig. 4-3b) if the deviatoric stress becomes larger than the threshold stress for brittle failure. Such failure occurs only at relatively shallow crustal depths above the brittle-ductile transition (see later, section 8-10). At deeper crustal levels, the pore space closes by crystalline creep and grain boundaries deform by ductile flow rather than through brittle failure (for details, see chapter six to eight).

□Exercise 4-2: The compressive total principal stresses at various crustal depths are: I) at 0 km, σ_1=-50 MPa, σ_2=0 MPa, σ_3=+50 MPa; II) at 4 km, σ_1=-150 MPa, σ_2=-100 MPa, and σ_3=-50 MPa; III) at 6 km, σ_1=-200 MPa, σ_2=-150 MPa, and σ_3=-100 MPa; IV) at 7 km, σ_1=-225 MPa, σ_2=-175 MPa, and σ_3=-125 MPa. a) Calculate the pressure at each depth, using the state of total stress, and compare it with that calculated from the lithostatic load, taking ρ=2,700 kg m^{-3}. b) Calculate the magnitude of the deviatoric stresses. c) Draw to scale three sections of the *principal planes* (see Fig. 4-4) of both the deviatoric and total stress ellipsoids. Indicate the direction of the stress arrows. Include a scaled circular section to represent the pressure. d) What is the direction of σ_2? How can you explain the origin of the large deviatoric stresses?

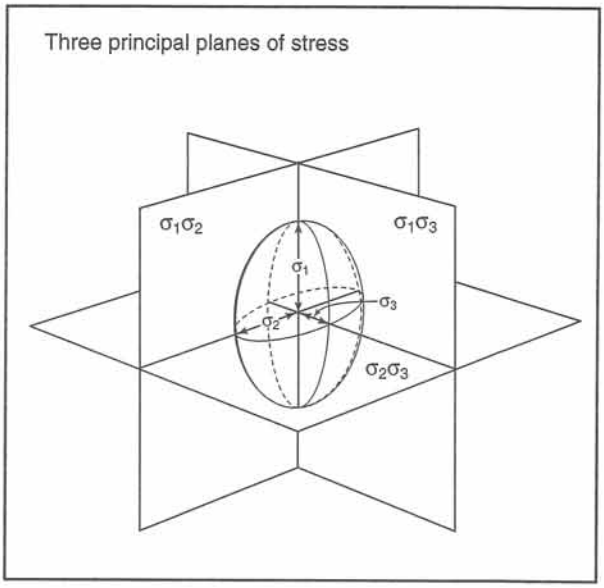

Figure 4-4: *Sketch of the three, mutually perpendicular, principal planes of stress. See exercise 4-2.*

4-3 Normal and shear stress

The magnitude of the three principal deviatoric stresses, $\tau_{1,2,3}$, and pressure, P, can be easily computed from three known principal stresses using expressions (4-2a) and (4-3). However, computation of the magnitude of the normal and shear components of either the total or deviatoric stresses, on an arbitrary plane inside a stressed continuum, is not so straightforward as that for normal and shear forces [c.f. eq. (3-3a & b)]. This is because the normal stress, σ_N, on any

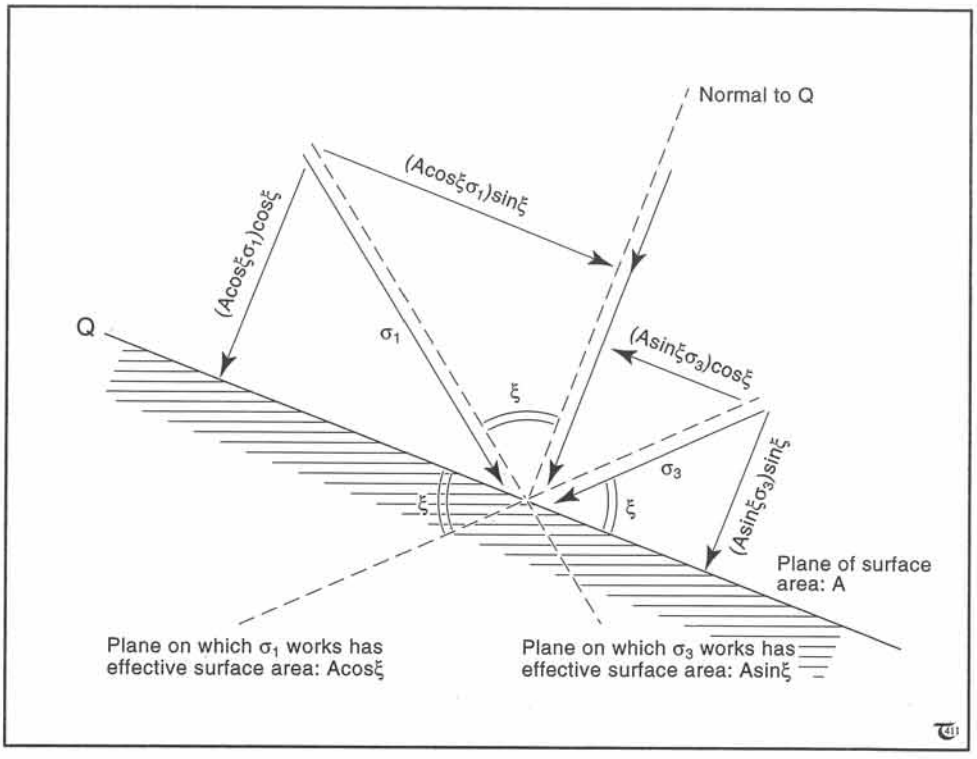

Figure 4-5: *Stress components, acting on arbitrary plane, Q, the normal of which is at angle ξ to the major principal stress, σ_1. Mohr's equations resolve the normal and shear stress on the plane.*

arbitrary inclined plane involves a change in surface area, A, on which the normal force is working, which needs to be taken into account in the calculation of the normal stress. The definition of stress as a force per unit area transforms it into a *tensor quantity*, due to which *the resultant stress can no longer be obtained by simple vector addition*. The *magnitude* of σ_1 is equal to F_{net}/A. The normal stress, σ_N, and the shear stress, σ_S, on the plane considered can be calculated from the *Mohr equations* (named so after the German engineer Otto Mohr who introduced the equations near the turn of the last century) (Fig. 4-5):

$$\sigma_N=[(\sigma_1+\sigma_3)/2]+[(\sigma_1-\sigma_3)/2]\cos 2\xi \qquad (4\text{-}5a)$$

which follows from $F_N=F_1\cos\xi+F_3\sin\xi$ and, thus, $\sigma_N A=(\sigma_1 A\cos\xi)\cos\xi+(\sigma_3 A\sin\xi)\sin\xi$;

$$\sigma_S=[(\sigma_1-\sigma_3)/2]\sin 2\xi \qquad (4\text{-}5b)$$

which follows from $F_S=F_1\sin\xi-F_3\cos\xi$ and thus $\sigma_S A=(\sigma_1 A\cos\xi)\sin\xi-(\sigma_3 A\sin\xi)\cos\xi$. For $\xi=45°$, equation (4-5b) is the same as equation (4-4).

The angle, ξ, indicated in Figure 4-5, is measured, within the plane of the two principal stresses, between the major principal stress and normal to the plane for which the normal and shear stresses are calculated. The Mohr equations are, also, valid for deviatoric, rather than the total stresses used here.

☐Exercise 4-3: Compare the set of equations (4-5a & b) and (3-3a & b), and explain the difference. How do the Mohr solutions differ from vector calculus solutions?

☐Exercise 4-4: Consider the syn-sedimentary slumping and liquefaction of sedimentary layers shortly after deposition which may cause so-called syn-sedimentary deformation of beds (Fig. 4-6). The physics of slumping is easy to understand, acknowledging the importance of pore pressure. Consider a sedimentary slope of loosely packed grains with ample pore space internally and a thick cover of aquiclude mud. a) Discuss why the slope will likely collapse when the ground water table rises. b) What is liquefaction, and how does it explain syn-sedimentary slumping?

Figure 4-6: *Slump-folds due to liquefaction of sediments shortly after deposition. Tortonian marl formation, Tabernas basin, southeast Spain.*

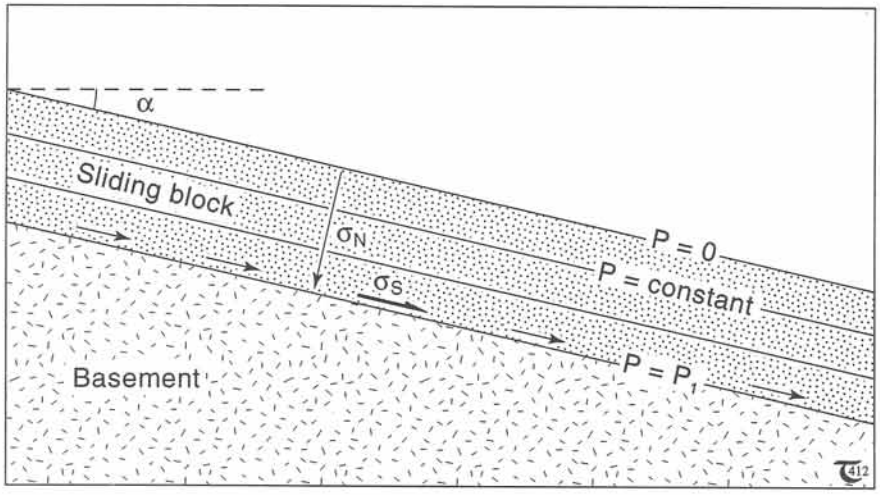

Figure 4-7: Principle sketch of potential slide mass resting at slope α with pure pressure, P, at the basal layer. See exercise 4-5.

□Exercise 4-5: Consider the gravity sliding of rock slabs. King Hubbert and William Rubey published, in 1959, an important study on the effect of fluid pressure in pores of rock at the base of potential slide masses (*Geological Society of America Bulletin*, volume 70, pages 115 to 166). It is simple to repeat their exercise. Consider a slab of rock with arbitrary length, resting on a slope as indicated in Figure 4-7. The pore pressure inside the basal layer is P. The coefficient of internal friction is μ=0.85. a) First take P=0. Consider the normal and shear stress at the base of the rock slab, and using eqs. (4-5a) & (4-5b), decide for which slope angles α the rock sheet is stable, critical, and unstable. b) Derive a general relationship between critical slope, α_c, and the normalized pressure, (P/σ_N), and graph the result in terms of α_c versus the normalized pressure, (P/σ_N). Remember, the presence of fluid pressure does not affect the magnitude of the shear stress but causes an apparent lowering of the normal stress. c) To initiate spontaneous gravitaty sliding on a shallow slope of only 2°, what normalized pressure is needed? d) If the pore pressure is zero, what additional shear stress needs to be applied externally to initiate gliding on subcritical slopes? Derive a general relationship between critical slope, α_c, and normalized tectonic shear stress, (τ_S/σ_N), and graph the result in terms of α_c versus the normalized tectonic shear stress, (τ_S/σ_N). Remember, the presence of tectonic shear stress does not affect the magnitude of the normal stress but causes an apparent increase of the shear stress. e) Combine the expressions resulting from (b) and (d), and construct one plot showing how both normalized pressure, (P/σ_N), and normalized tectonic shear stress, (τ_S/σ_N), affect the critical slope, α_c.

4-4 Mohr circle of stress

The *Mohr circle* is a simple nomogram or method to construct graphically the shear and normal stress components on a plane of arbitrary orientation, ξ, provided σ_1 and σ_3 (or τ_1 and τ_3) are known (Fig. 4-8a). Two perpendicular axes are constructed. The vertical axis is scaled for the shear stress; the horizontal axis is similarly scaled for the normal stress (Fig. 4-8b). The magnitudes of the two known principal stresses, σ_1 and σ_3, are then plotted along the horizontal axis, and the center for the Mohr circle is located along the horizontal axis between σ_1 and σ_3. The practical purpose of the Mohr circle is that the magnitude of the normal stress, σ_N, and the shear stress, σ_S, on the plane of orientation, ξ, can be read from the two axes. The reading is done for point Q, located on the circle, in a position determined by the double angle, 2ξ, measured in an anti-clockwise direction from the horizontal scale. Figure 4-8c graphs the variation in both the total normal and the shear stress against ξ as simple goniometric functions, given in eqs. (4-5a) & (4-5b).

The Mohr equations and the associated nomogram for deviatoric stresses in two dimensions is much simpler, because it follows from equations (4-2b) and (4-3) that τ_1 is always equal to $-\tau_3$. Consequently, the Mohr equations for deviatoric stress simplify to:

$$\tau_N=[(\tau_1-\tau_3)/2]\cos 2\xi=\tau_1\cos 2\xi \qquad (4\text{-}6a)$$
$$\tau_S=[(\tau_1-\tau_3)/2]\sin 2\xi=\tau_1\sin 2\xi \qquad (4\text{-}6b)$$

Figure 4-9a shows the corresponding *Mohr diagram for deviatoric stress* in two dimensions. An alternative method, perhaps more practical than the Mohr circle, directly plots the variation, in both the normal and the shear stress against ξ, as a simple goniometric function (Fig. 4-9b).

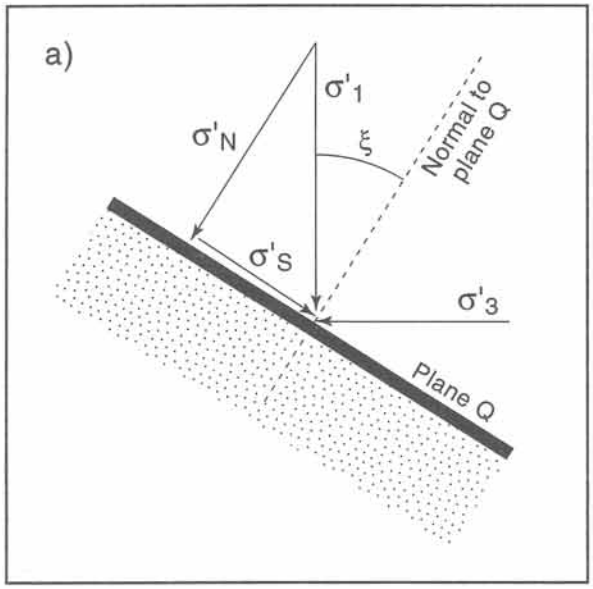

Figure 4-8a: Situation sketch for Mohr diagram.

☐Exercise 4-6: a) Construct a Mohr diagram to find σ_N and σ_S on planes at 30° and 45° to the σ_1-direction at 4 km depth in the example of exercise 4-2. b) Subtract the pressure, and find τ_N and τ_S on planes at 30° and 45° to the τ_1-direction at 4 km depth.

☐Exercise 4-7: Construct a Mohr diagram to find the magnitudes and orientations of σ_1 and σ_3 from known σ_N and σ_S on two perpendicular planes in the same material point studied. On plane (1): σ_N=220 MPa and σ_S= 110 MPa; on plane (2): σ_N=120 MPa and σ_S=-110 MPa.

☐Exercise 4-8: Use a Mohr circle to demonstrate that: a) the shear stress on any two perpendicular planes is always equal in magnitude but opposite in sense and b) the sum of normal stresses on any two perpendicular planes is constant for a given state of stress.

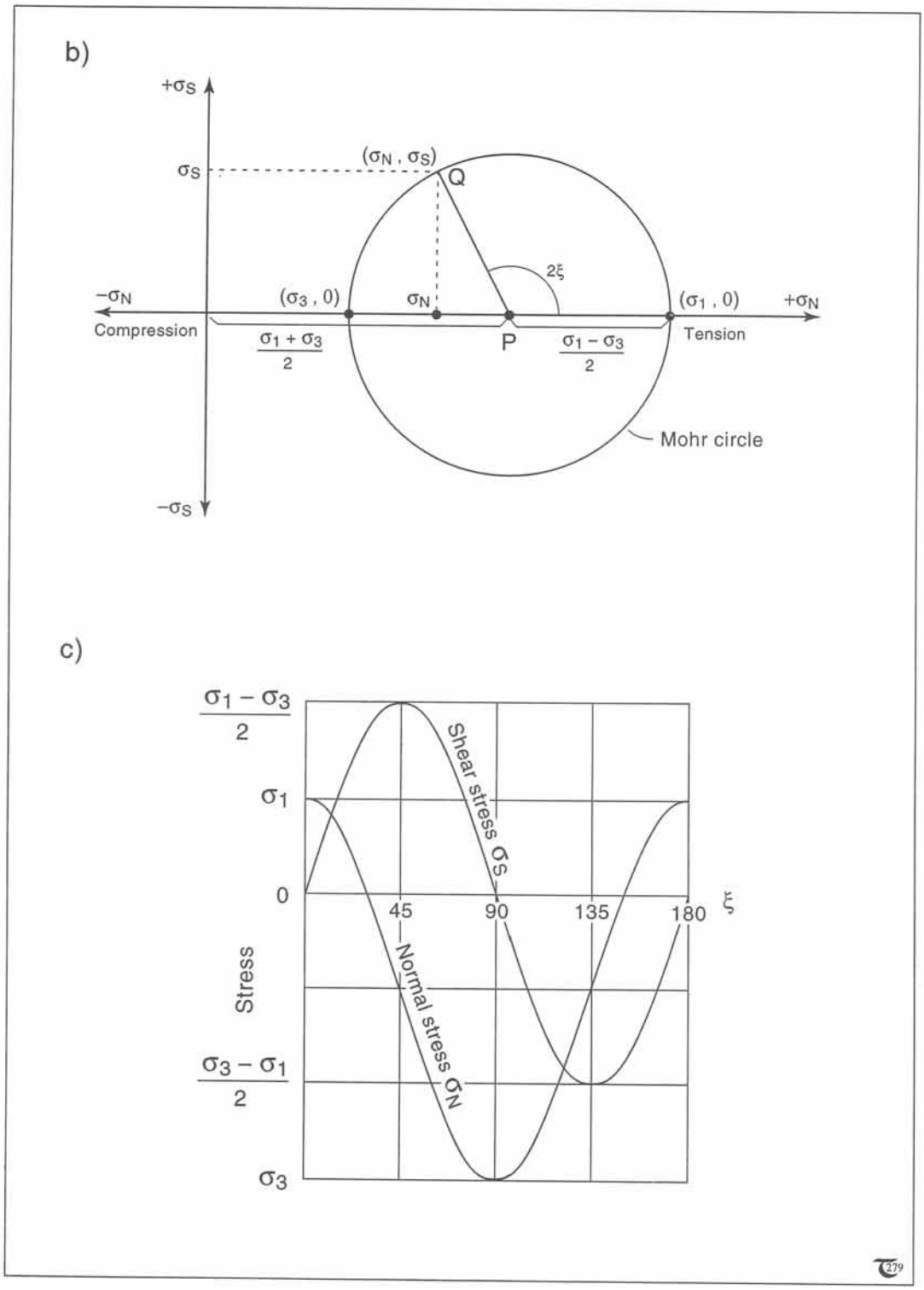

Figure 4-8b & c: *b) Mohr circle for total stress (see text). c) Relative magnitude of shear stress and normal stress for plane orientations, ξ. The pressure, P, is equal to* $(\sigma_1+\sigma_3)/2$.

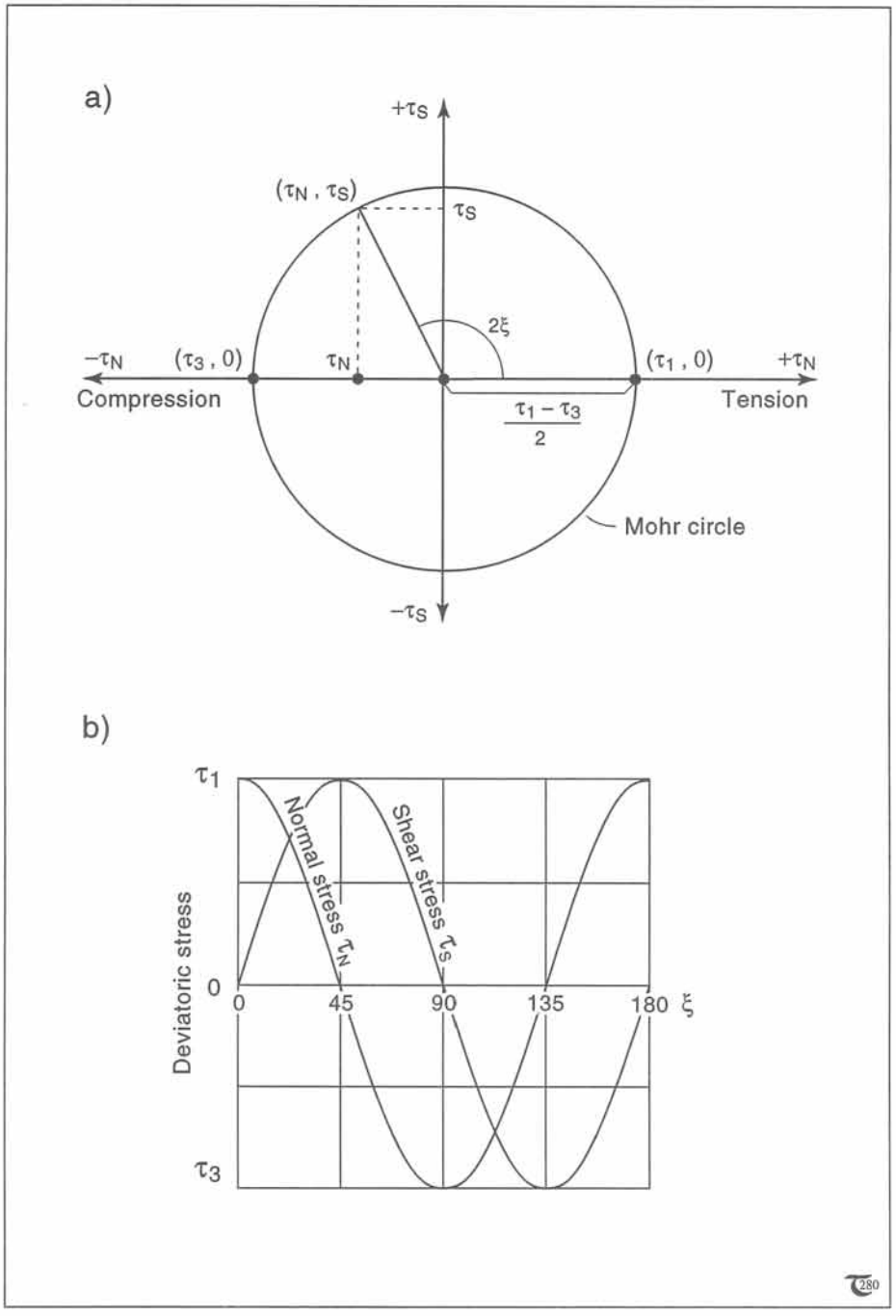

Figure 4-9: *a) Mohr circle for deviatoric stress. b) Relative magnitude of normal and shear stress.*

4-5 Force and stress orientation

A complication, often little emphasized, if not neglected, in the literature, is that *the major principal stresses, σ_1 and τ_1, usually are not parallel to the net force vector, F_{net}.* This can be demonstrated as follows: Consider first a granite block, resting on a horizontal plane (Fig. 4-10a). In this case, the vectors of τ_1, σ_1, and the gravitationally induced F_{net} are parallel. However, this will not be so for stresses at the basal plane of a granite block on an inclined slope (Fig. 4-10b). This becomes apparent, comparing equations (3-3a & b) for vector calculation of force magnitudes and equations (4-6a & b) for tensor calculation of stress magnitudes. The normal and shear stresses on a plane of area A and inclination α have orientations which coincide with the vectors of the normal and shear forces, and their magnitudes are given by $\tau_N=(F_N/A)-P$ and $\tau_S=(F_S/A)-P$. Combining equations (3-3a & b) with (4-6a & b) yields:

$$\tau_N=[(F_{net}/A)-P]\cos\alpha=\tau_1\cos 2\xi \qquad (4\text{-}7a)$$
$$\tau_S=[(F_{net}/A)-P]\sin\alpha=\tau_1\sin 2\xi \qquad (4\text{-}7b)$$

It can now be concluded that the *orientations* of τ_1 (fixed by ξ) and F_{net} (fixed by α, if F_{net} is due to gravity) are related by (Fig. 4-11):

$$\alpha=2\xi \qquad (4\text{-}8)$$

where the angle, ξ, is measured between the principal stresses, τ_1 (or σ_1), and the normal to the plane of shear stress and α is the slope of the plane.

☐Exercise 4-9: Consider the difference between a stress and force orientation by comparing the plots of exercise 3-3c with the graph in Figure 4-9b. a) For which slope α is the shear stress at maximum? What is the magnitude of the shear force for this slope? b) For which slope α is the normal stress at maximum? What is the magnitude of the normal force for this slope? c) Calculate and sketch the orientation of σ_1 and F_{net} on the slope, α, for maximum shear stress and minimum normal stress.

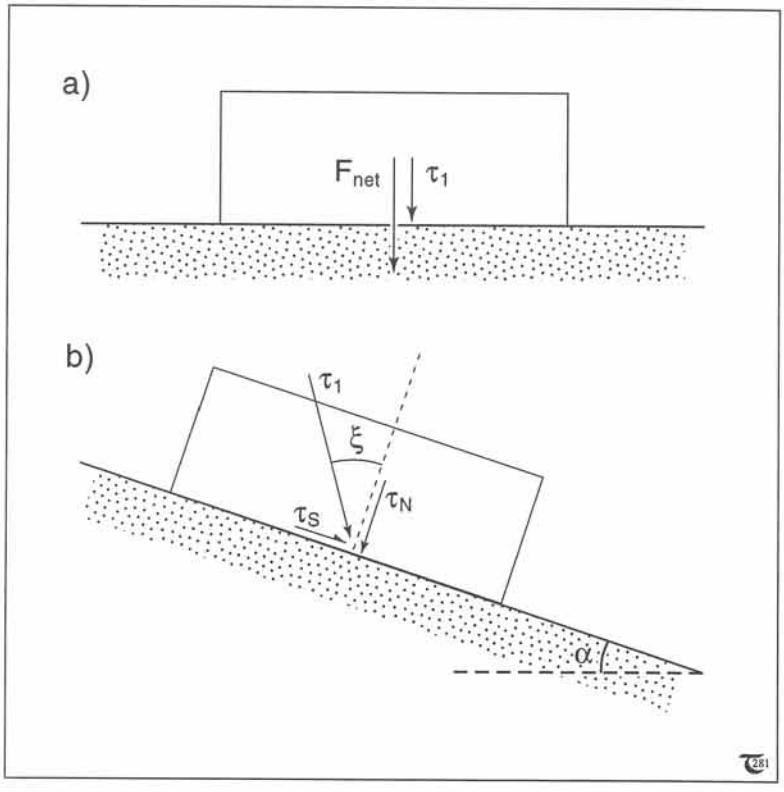

Figure 4-10a) & b): *a) The major principal stress, τ_1, on the base of a horizontal plane, loaded by overlying rocks, is parallel to the force vector, F_{net}. b) On a sloping surface, the net load force and the major principal stress are no longer parallel. Figure 4-11 and the text explain why.*

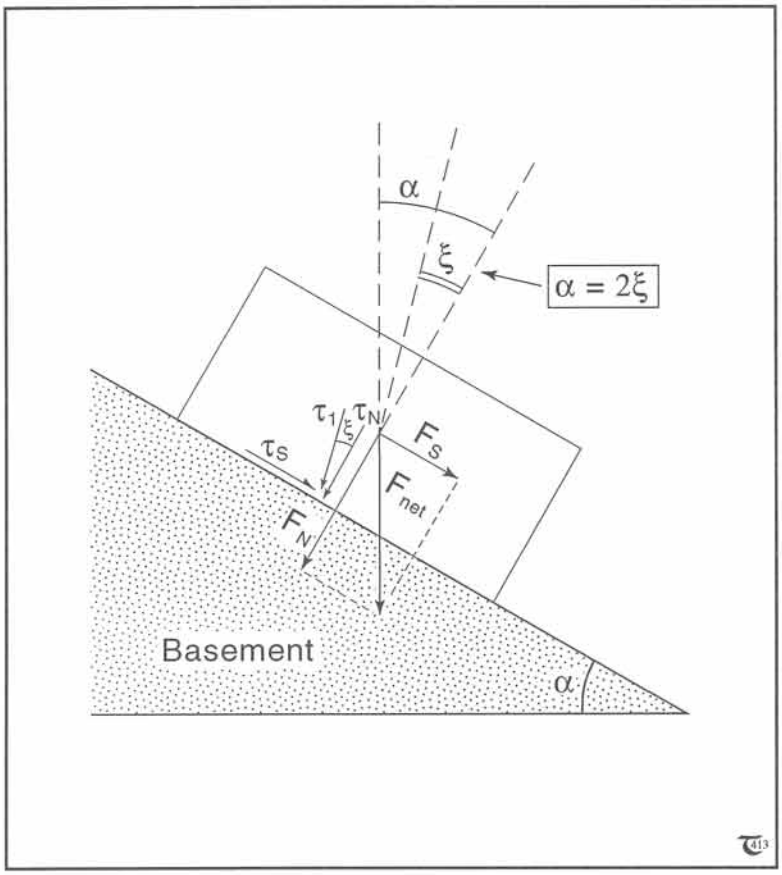

Figure 4-11: The angular relationship between a gravitational load force, F_{net}, and the major principal stress on a plane inclined at angle α. See equation (4-8).

4-6 Stress trajectories and intrusions

The state of stress in a point can be represented by a stress ellipsoid, which fixes the relative magnitude of the three axes of the principal stress. If the three principal stress axes inside a material are similarly oriented in each point of the material, the stress field is *uniform*. A simple fashion to display graphically the spatial variation or absence of variation in the orientation of the principal stress axes makes use of a set of orthogonal gridlines, representing the principal stress directions: *stress trajectories*. The stress trajectories for a *uniform stress field* are an orthogonal set of *straight gridlines*. The orientation of the stress axes inside a material does not necessarily need to maintain a uniform orientation throughout that material. Stress trajectories for a *non-uniform stress field* integrate the principal stress directions into an orthogonal set of *smoothly curved gridlines*.

Figure 4-12a illustrates the trajectories of the principal stress in a vertical plane through the center of an axisymmetric subsurface dome of either salt or magma, considering only the stresses arising from the pressurized dome. The pressure on the walls of the dome is a surface force, which causes deviatoric and associated total stresses inside the host rock, as shown. The σ_3-trajectories, *outside* the dome area, are always perpendicular to the vertical plane of section, and visualized are the σ_1- and σ_2-trajectories. The vertical plane *above* the dome contains the σ_1- and σ_3-trajectories and is itself normal to σ_2. The points where σ_2 and σ_3 have the same magnitude, so that their axial orientation becomes indistinguishable, are termed *isotropic points* or *neutral points*, if both stresses are larger than zero, and *singular points*, if they are both equal to zero. Figures 4-12b & c illustrate the stress trajectories in horizontal planes through the dome at one and two kilometers depth, respectively. The sections of Figure 4-12b are complementary to those shown in Figure 4-12a, and together they visualize the variation in the orientation of the three principal stress axes in three-dimensional space.

An important property of principal stress trajectories is that *a trajectory must either end parallel or perpendicular to a surface free of shear stress*. In the example of Figure 4-12, the ground surface is free of any shear stress. Also the walls of the pressured dome are free from a shear stress, because only a pressure, which is equal in all directions without generating any shear stress, is exerted. It is worth noting that the

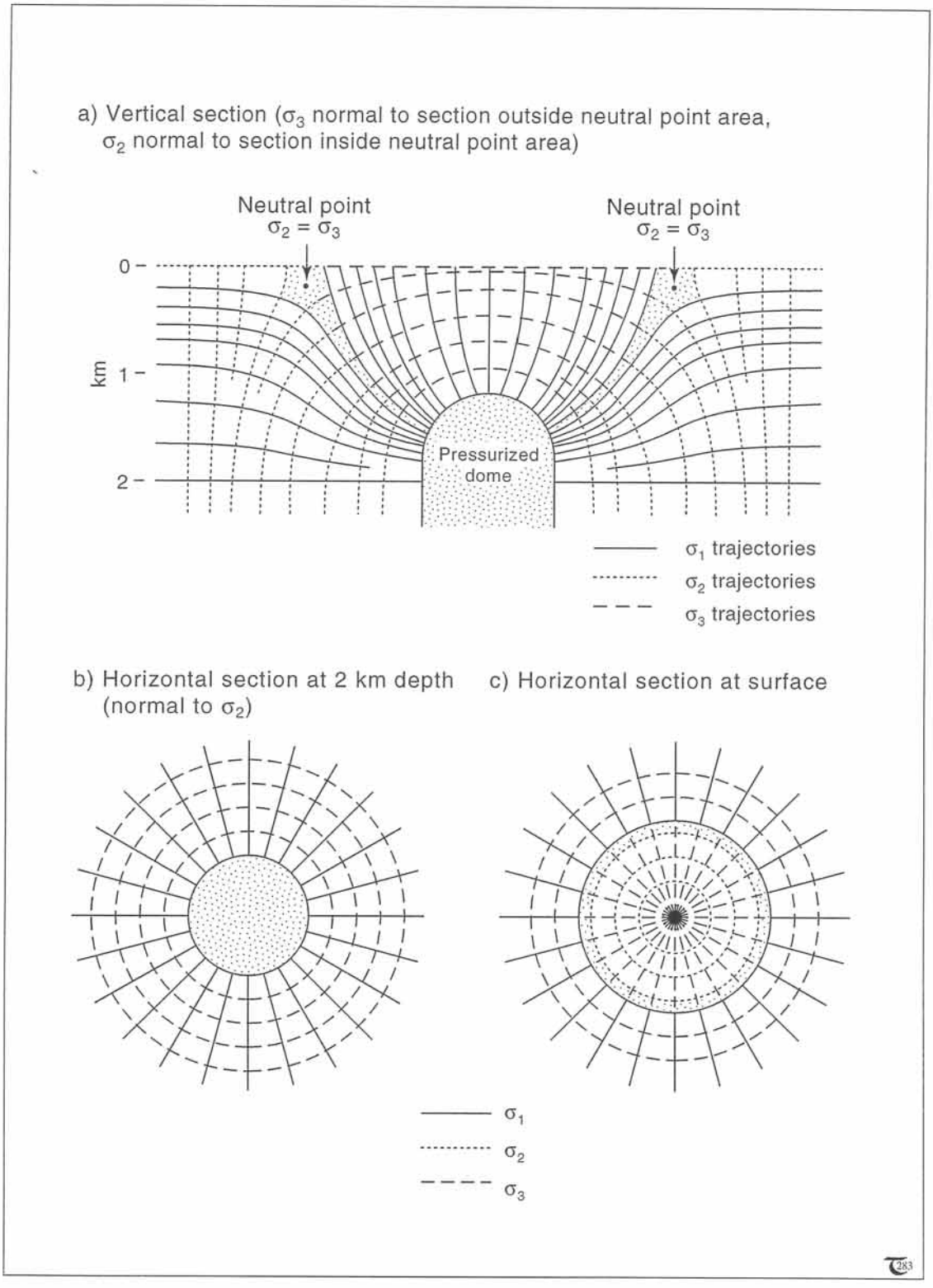

Figure 4-12: *a) Stress trajectories in vertical section, parallel to the symmetry axis of a pressurized dome, b) & c) normal to the symmetry axis.*

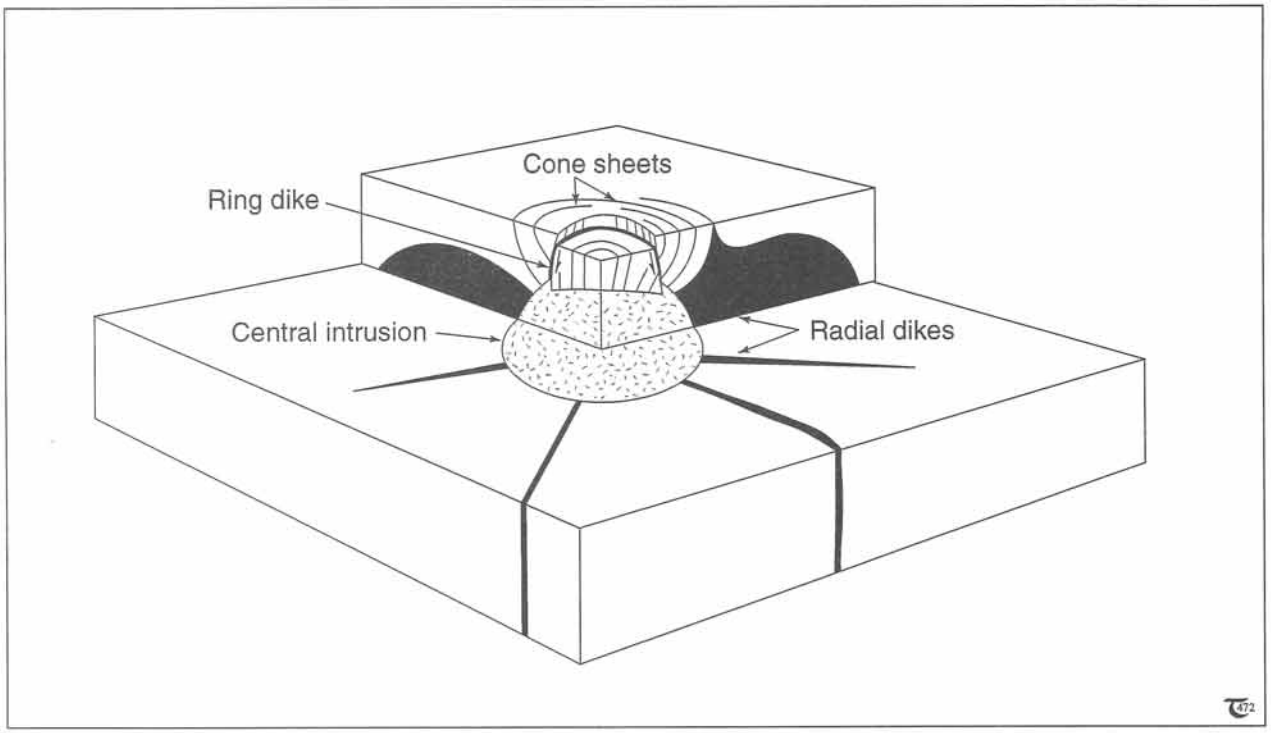

Figure 4-13: *Block diagram of an igneous dome, showing common features, such as radial dikes, ring dikes, and cone sheets.*

stress trajectories are orthogonal to the walls of the solid rock, if free of shear stress. However, the pressure is, also, a surface force for the host rock and causes stress gradients, as outlined by the trajectories. Using the geometrical constraint of mutual orthogonality and orthogonality to shear stress-free boundaries, it is quite simple to estimate the likely stress trajectory pattern, arising in simple, isothermal mechanics.

Stress trajectories are extremely useful in geological applications, involving dike intrusion and shear faulting. *Intrusion* of pressurized material, whether hot magma, pressurized ductile salt, or clay, is most likely to succeed within σ_1-σ_2 surfaces, perpendicular to the least principal stress axis. The trace of the σ_1-σ_2 surfaces is outlined by the σ_2-trajectories in Figure 4-12a and by the σ_1-trajectories in Figure 4-12b. Figure 4-13 shows the likely intrusion pattern, resulting from this stress field.

□Exercise 4-10: Consider the relationship between stress trajectories and intrusive structures. Ship Rock is a striking high-relief feature, interrupting the relatively low-relief landscape of New Mexico (Fig. 4-14). The Rock, in fact, is the remnant of the central intrusion pipe underneath a Tertiary volcano, which has now been removed by erosion. From the pipe emerge, at least, three subvertical radial dikes, clearly visible on aerial pictures. Sketch a horizontal trajectory map likely for the paleostress in the country rock at the time of dike emplacement.

Figure 4-14: *Ship Rock Mountain, a landmark in the desert of New Mexico. The explacement of the radial dikes can be understood in terms of stress trajectories. See exercise 4-10. Courtesy John Shelton.*

☐Exercise 4-11: The orientation of potential intrusions can be predicted from the stress trajectories. The Richat Dome, Mauritania, is a beautiful, axially symmetric, shallow dome of 60 km diameter, exposing concentric rings of outward dipping, alternately competent and incompetent, sedimentary rocks (Fig. 4-15). Assume that the dome is due to a buoyant, granitic pluton underneath. a) Sketch the principal paleostress trajectories in the area at ground level for the time of the dome formation. b) Predict the orientation of the pegmatite dikes found in the Richat area.

Figure 4-15: *Oblique photograph, by Gemini astronaut, of the Richat Dome, Mauritania. The area enclosed by the outer layer of rim rock is approximately sixty kilometers in diameter. See exercise 14-11.*

☐Exercise 4-12: a) Sketch the stress pattern, suggested by the fault pattern over the Clay Creek Dome, Texas (Fig. 4-16a). b) Sketch the stress pattern, suggested by the fault pattern over the Bell Isle Dome, Louisiana (Fig. 4-16b). c) Argue why the stress pattern implied by the Clay Creek Dome is radially symmetric and that of the Bell Isle Dome is not.

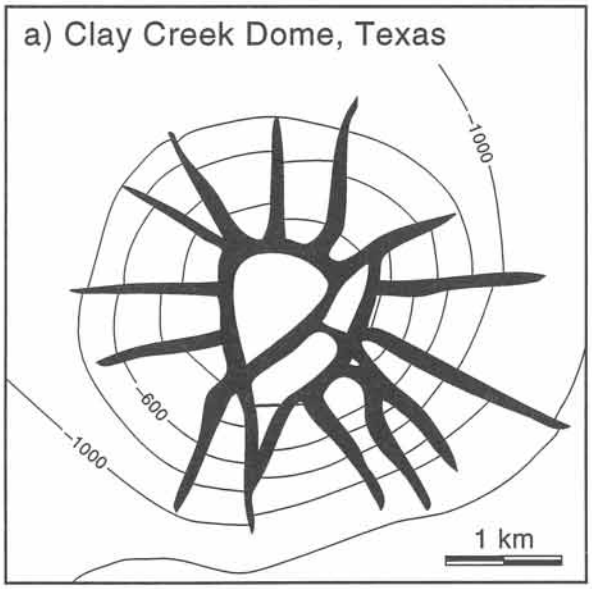

Figure 4-16a: Pattern of subsurface faults around Clay Creek Dome, USA. See exercise 4-12.

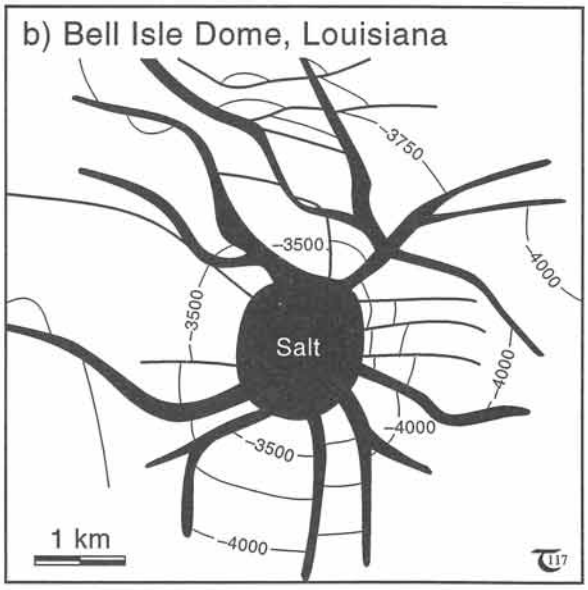

Figure 4-16b: Pattern of subsurface faults around Bell Isle Dome, USA. See exercise 4-12.

4-7 In-situ stress measurements

It is relatively straightforward to measure the present-day stresses in rocks using two principal methods: hydrofracturing and overcoring. *Hydrofracturing* pumps up inflatable packers against the wall of a drill hole until the rock fractures. Fractures are assumed to open in the direction of the σ_1-σ_2 plane so that the orientation of σ_3 is found perpendicular to the fracture. The magnitude of σ_3 is assumed equal to the hydraulic pressure required to open the crack. The orientation of the bore hole is of great influence on the accuracy of the results; repetition of the measurements in bore holes at right angles helps to constrain both the magnitude and orientation of the three principal stresses.

Overcoring is a more involved technique, where a drill hole is made and strain gauges are emplaced. It is assumed that the stress in the direction of the strain gauge is not affected by the hole itself. The strain gauges are not able to measure anything in this hole as such because of instantaneous elastic displacements of the walls controlled by the stress field. However, the walls would resume their unstressed shape if the outside stress could be removed, and the associated recovery of elastic strain is a measure of the stress magnitude (see chapter five). The release of

the tectonic stress is achieved by cutting an annular hole with an inner radius larger than that of the initial drill hole. In this fashion, a rim of rock is preserved around the hole in which the strain gauges now record the elastic recovery of the wall rock. Again, the orientation of the drill hole is of important significance to the accuracy of the results. The principal stresses can be calculated from the normal stresses on the walls of the drill hole, using the Mohr equations, as applied in exercise 10-13 (chapter 10, page 171).

Relatively little attention has been paid to methods of *paleostress* determination, using past deformation structures, preserved in rocks, to recover the principal stresses at the time the deformation took place. The estimation of paleostress *magnitudes* is likely to remain rather conjectural because of the uncertainty about the physical conditions prevailing at the time of deformation. However, paleostress *directions* sometimes can be constrained using the stress trajectory principles outlined in section 4-6.

□Exercise 4-13: The horizontal stress pattern about the salt dome of Figure 4-17 is not radially symmetric at all. a) Draw the stress trajectories on Figure 4-17. b) Explain what may be the cause of this deviation from the model in Figure 4-12c.

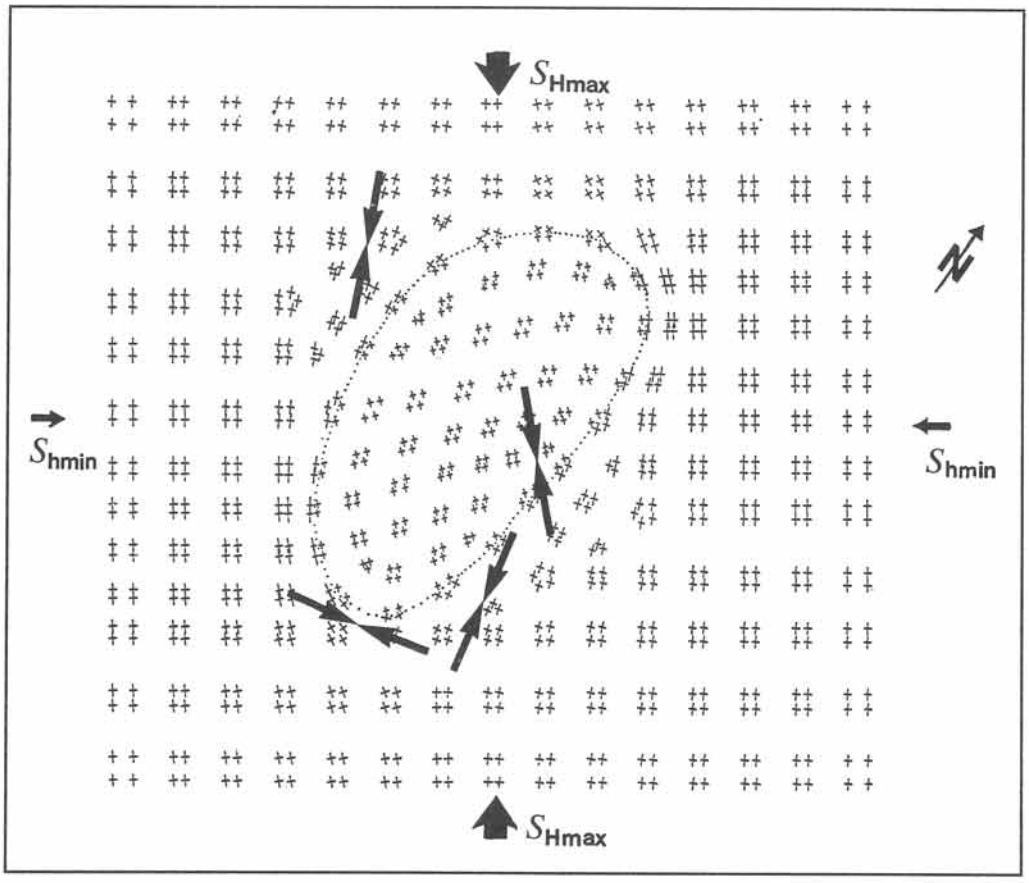

Figure 4-17: *Principal stress orientations in horizontal section of an elliptical salt dome, north Germany. Generated by a finite-element model, calibrated by in-situ stress measurements (fat arrows).*

References

A. Books

Tectonic Stress in the Lithosphere (1991, Philosophical Transactions of the Royal Society of London, series A, volume 337 (no. 1645), pages 1 to 194), edited by Whitmarsh, Bott, Fairhead, and Kusznir. Contains an instructive set of research papers on lithospheric stress, presented at a 1991-meeting of the *Royal Society of London*.

Stress Regimes in the Lithosphere (1992, Princeton University Press, 457 pages), by Terry Engelder. This account on stress in the lithosphere includes detailed discussions on a range of methods for in-situ stress measurements.

B. Articles

The classical theory on the effect of pore pressure in thrust sheets, now reproduced by you in exercise 4-4, was originally published in the following two companion papers:

Hubbert, K. and Rubey, W.W. (1959, *Geological Society of America Bulletin*, volume 70, pages 115 to 166). Role of fluid pressure in mechanics of overthrust faulting, I.

Rubey, W.W. and Hubbert, K. (1959, *Geological Society of America Bulletin*, volume 70, pages 167 to 206). Role of fluid pressure in mechanics of overthrust faulting, II.

An inspiring example of a world stress map with a short discussion on its assumptions and implications was published in the following paper:

Mary and Mark Zoback and others (27 more coauthors), (1989, *Nature*, volume 341, pages 291 to 298). Global Patterns of Tectonic Stress.

A new method for estimating the principal paleostress *orientation* from ductile deformation structures is outlined in the following article:

Weijermars, R. (1993, *Geological Society of America Bulletin*, volume 105, pages 1,491 to 1,510). Estimation of paleostress orientation within deformation zones between two mobile plates.